Inorg. Chem. **2006**, *45*, 6235–6245

Degradation of Ionized $OV(OCH_3)_3$ in the Gas Phase. From the Neutral Compound All the Way down to the Quasi-terminal Fragments VO^+ and VOH^+†

Detlef Schröder,*,‡,§ Marianne Engeser,|| Helmut Schwarz,§ Esther C. E. Rosenthal,‡ Jens Döbler,⊥ and Joachim Sauer⊥

Institute for Organic Chemistry and Biochemistry, Czech Academy of Sciences, 16610 Prague 6, Czech Republic, Institut für Chemie der Technischen Universität Berlin, Strasse des 17 Juni 135, D-10623 Berlin, Germany, Kekulé-Institut für Organische Chemie und Biochemie, Gerhard-Domagk-Strasse 1, D-53121 Bonn, Germany, and Institut für Chemie der Humboldt Universität Berlin, Unter den Linden 6, D-10099 Berlin, Germany

Received January 26, 2006

The consecutive fragmentation of ionized trimethyl vanadate(V), $OV(OCH_3)_3$ (**1**), is examined by experiment and theory. After an elimination of formaldehyde from the molecular ion $\mathbf{1}^+$, subsequent dissociations proceed via losses of first H_2 and then two molecules of formaldehyde to finally yield the VOH^+ cation; these redox reactions involve the V^{II}/V^{IV} manifold. At elevated energies, expulsion of $CH_3O^\bullet$ from $\mathbf{1}^+$ can efficiently compete to afford $OV(OCH_3)_2^+$, a formal V^V compound, from which subsequent losses of H_2 and two units of CH_2O lead to bare VO^+, thereby exploring the V^{III}/V^V redox manifold. Experiments using complementary mass spectrometric techniques, i.e., neutralization–reionization experiments and ion/molecule reactions, in conjunction with extensive computational studies provide deep insight into the ion structures and the relative energetics of these dissociation reactions. In particular, a quantitative energetic scheme is obtained that ranges from neutral $OV(OCH_3)_3$ all the way down to the quasi-terminal fragment ions VOH^+ and VO^+, respectively.

1. Introduction

Mass spectrometric studies of small, coordinatively unsaturated transition-metal fragments have provided detailed insight into the thermochemistry and reactivities of these particular species. This knowledge encompasses thermochemical data on metal−ligand bond strengths, different effects of ligands, aspects of various kinds of C−H−, C−C−, and C−X (X = heteroatom) bond activations, as well as insight into the elementary steps of oxidation catalysis.[1,2] Another important aspect of these studies on the gas-phase chemistry of transition-metal fragments concerns the close interaction with theory, which nowadays is capable of handling these systems reasonably well.

Quite often, however, there exists a considerable gap between observations made in condensed matter and the implications derived from gas-phase studies. Part of this gap is due to the different degrees of coordination of the reactive species that exist in both environments. In the gas phase, where often coordinatively highly unsaturated species are formed, it is relatively easy to accurately determine the properties of these reagents, e.g., the highly reactive FeO^+ cation,[3−5] whereas mounting difficulties are encountered as the size of the system and thus the degree of ligation increase. In the condensed phase, the properties of bulk substances—usually coordinatively saturated ones—can be determined

† Dedicated to Professor Dieter Enders on the occasion of his 60th birthday.

* To whom correspondence should be addressed. E-mail: detlef.schroeder@uochb.cas.cz.

‡ Czech Academy of Sciences.

§ Institut für Chemie der Technischen Universität Berlin.

|| Kekulé-Institut für Organische Chemie und Biochemie.

⊥ Institut für Chemie der Humboldt Universität Berlin.

(1) Armentrout, P. B. *Int. J. Mass Spectrom.* **2003**, *227*, 289.

(2) Böhme, D. K.; Schwarz, H. *Angew. Chem.* **2005**, *117*, 2388; *Angew. Chem., Int. Ed.* **2005**, *44*, 2336.

(3) Schröder, D.; Schwarz, H. *Angew. Chem.* **1995**, *107*, 2126; *Angew. Chem., Int. Ed. Engl.* **1995**, *34*, 1973.

(4) Schröder, D.; Shaik, S.; Schwarz, H. Metal−Oxo and Metal−Peroxo Species in Catalytic Oxidations. In *Structure and Bonding*; Meunier, B., Ed.; Springer: Berlin, 2000; Vol. 97, p 91.

(5) Metz, R. B.; Nicolas, C.; Ahmed, M.; Leone, S. R. *J. Chem. Phys.* **2005**, *123*, 114313 and references cited therein.

10.1021/ic060150w CCC: $33.50
Published on Web 07/06/2006

easily, and also unsaturated 14- or 16-electron complexes can be examined by several techniques. The gap thus arises from the intermediate region of partially ligated transition-metal complexes, which are considered as the reactive intermediates involved in numerous chemical transformations.

In a previous paper,[6] we have described photoionization experiments with gaseous trimethyl vanadate(V), $OV(OCH_3)_3$ (**1**), and the primary fragmentation channels of the molecular cation $\mathbf{1}^+$. In this paper, we attempt to use the gas-phase ion chemistry of **1** in order to link the properties of the neutral compound with the quasi-terminal ionic fragments VO^+ and VOH^+ obtained upon consecutive degradation of gaseous $\mathbf{1}^+$. To this end, various mass spectrometric experiments are complemented by quantum chemical calculations employing density functional theory (DFT), where some of the limitations of the different approaches used can be surmounted by virtue of their combination.

2. Experimental and Theoretical Methods

Several experiments using sector-field mass spectrometry as well as photoionization techniques have been described in a previous publication about the gas-phase chemistry of $OV(OCH_3)_3$. In addition, the ion/molecule reactions of V^+, VO^+, VOH^+, and VO_2^+ with methanol have been investigated by ion-cyclotron resonance (ICR) mass spectrometry[7,8] as well as multipole techniques.[9] Here, some complementary experiments are described that were performed using a VG BIO-Q mass spectrometer,[10] which consists of an electrospray ionization (ESI) source combined with a tandem mass spectrometer of QHQ configuration (Q stands for quadrupole and H for hexapole). In the present experiments, millimolar solutions of either $OVSO_4$ in water/methanol (1:1) or $OV(OCH_3)_3$ in pure methanol were introduced through a stainless steel capillary to the ESI source via a syringe pump (2−5 μL/min). Nitrogen was used as a nebulizer and as a drying gas at a source temperature of 100 °C. Optimal yields of the desired V-containing cations were achieved by adjusting the cone voltage between 5 and 180 V. At low cone voltages, multiply ligated ions prevail, e.g., formal $[OV(OCH_3)(CH_3OH)_3]^+$ (m/z = 194) from $OVSO_4$ and $[OV(OCH_3)_2(CH_3OH)_2]^+$ (m/z = 193) from $OV(OCH_3)_3$, whereas successive dissociations occur at higher cone voltages (see below). For collision-induced dissociation (CID), the ions of interest were mass-selected using Q1, interacted with Xe as a collision gas in the hexapole under single-collision conditions (typically 3×10^{-4} mbar) at variable kinetic energies (E_{lab} = 0−20 eV), while scanning Q2 to monitor the ionic products. Likewise, ion-reactivity studies were performed using D_2O, CD_3OD, and CH_3OCH_3 as reagent gases at E_{lab} nominally set to 0 eV. Most of the products formed in the reactions with these neutral molecules rapidly decline at elevated collision energies, thereby justifying the assumption that these processes occur at quasi-thermal energies. To probe the occurrence of consecutive ion/molecule reactions, the neutral molecules' pressures were deliberately also adjusted to reach the multiple-collision regime.

For a semiquantitative description of the energy-dependent CID spectra,[11] the threshold behaviors were empirically analyzed by fitting sigmoid functions of the type $I_i(E_{CM}) = BR_i/(1 + e^{(E_{1/2,i}-E_{CM})b_i})$ to the observed relative fragment-ion intensities using a least-squares criterion. Here, BR_i stands for the branching ratio of a particular product ion ($\sum BR_i = 1$), $E_{1/2,i}$ is the energy at which the sigmoid function has reached half of its maximum, E_{CM} is the collision energy in the center-of-mass frame [$E_{CM} = E_{lab}m_T/(m_T + m_I)$, where m_T and m_I stand for the masses of the neutral target gas and of the ion, respectively, and E_{lab} is the collision energy in the laboratory frame], and the phenomenological parameter b_i describes the rise of the sigmoid curve. In consecutive dissociations, all secondary product ions were summed to the primary fragments. Further, contributions of nonnegligible ion decay at E_{lab} = 0 eV as well as the fraction of nonfragmenting parent ions at large collision energies (due to the single collision conditions maintained) were acknowledged by means of scaling and normalization. As shown earlier, this physically reasonable, though empirical, approach is able to reproduce the measured ion abundances quite well.[11] It is important to note, however, that the term $E_{1/2}$ used in the exponent does not correspond to the intrinsic thermochemical threshold of the fragmentation considered.

For a complementary characterization of $[VCH_3O_2]^+$ species formed in the course of the consecutive fragmentation of $\mathbf{1}^+$, neutralization−reionization (NR) experiments[12,13] were performed using a modified VG ZAB/HF/AMD 604 four-sector mass spectrometer of the BEBE configuration (B stands for the magnetic sector and E for the electric sector),[14] which has already been used in our previous study of $OV(OCH_3)_3$. The ions of interest were generated by electron ionization (70 eV) of **1** and the fully deuterated compound $\mathbf{1_D}$, respectively. After acceleration to 8 keV of kinetic energy, NR spectra were acquired by (i) mass selection of the $[VCH_3O_2]^+$ species of interest by means of B(1) and E(1), (ii) collisional neutralization with Xe at ca. 80% transmission (T), (iii) removal of all charged species by means of a deflector electrode, (iv) reionization in a collision with O_2 (80% T), and (v) mass analysis of the cationic species formed by means of B(2); the fourth sector, E(2), was not used in this study. The spectra were accumulated with the AMD-Intectra data systems, and ca. 30 scans were averaged to improve the signal-to-noise ratio.

(6) Schröder, D.; Loos, J.; Engeser, M.; Schwarz, H.; Jankowiak, H.-C.; Berger, R.; Thissen, R.; Dutuit, O.; Döbler, J.; Sauer, J. *Inorg. Chem.* **2004**, *43*, 1976.
(7) Cao, Y.; Zhao, X.; Xin, B.; Xiong, S.; Tang, Z. *J. Mol. Struct. (THEOCHEM)* **2004**, *683*, 141.
(8) Engeser, M.; Schröder, D.; Schwarz, H. *Chem.—Eur. J.* **2005**, *11*, 5975.
(9) Justes, D. R.; Moore, N. A.; Castleman, A. W., Jr. *J. Phys. Chem. B* **2004**, *108*, 3855.
(10) Schröder, D.; Weiske, T.; Schwarz, H. *Int. J. Mass Spectrom.* **2002**, *219*, 729.
(11) Schröder, D.; Engeser, M.; Brönstrup, M.; Daniel, C.; Spandl, J.; Hartl, H. *Int. J. Mass Spectrom.* **2003**, *228*, 743.
(12) Tureček, F. *Top. Curr. Chem.* **2003**, *225*, 77.
(13) Schalley, C. A.; Hornung, G.; Schröder, D.; Schwarz, H. *Chem. Soc. Rev.* **1998**, *27*, 91.
(14) Schalley, C. A.; Schröder, D.; Schwarz, H. *Int. J. Mass Spectrom. Ion Processes* **1996** *153*, 173.

Scheme 1

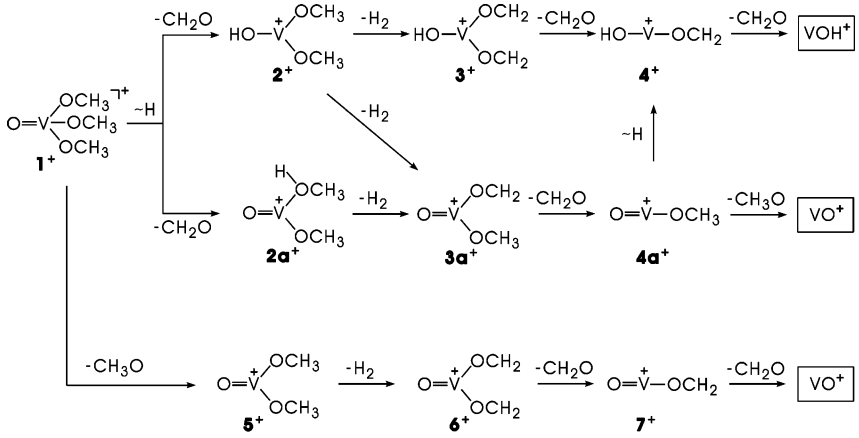

A few additional experiments were performed with a Spectrospin CMS 47X Fourier transform ICR (FTICR) mass spectrometer equipped with an external ion source.[15,16] In brief, V^+ was generated by laser ablation of a V target using a Nd:YAG laser operating at 1064 nm, transferred to the ICR cell positioned in a 7.05-T superconducting magnet, mass-selected, and converted to VO^+ using O_2. After another mass selection, the latter ion was allowed to react with the neutral molecules of interest at stationary pressures on the order of 10^{-8} mbar. During this procedure, the ions undergo several hundreds of collisions such that the product ions are assumed to be thermalized.[17] The experimental second-order rate constants are evaluated assuming the pseudo-first-order kinetic approximation after calibration of the measured pressures and acknowledgment of the ion gauge sensitivities;[18] the error of the absolute rate constants is ±30%. Likewise, the reactivities of the major product ions formed in the experiments are monitored after mass selection as described above.

All theoretical studies employed the hybrid density functional B3-LYP[19,20] implemented in Turbomole 5.5.[21,22] Geometric structures were optimized in all-electron Kohn−Sham calculations employing Ahlrichs' valence triple-ζ basis sets with polarization functions on all atoms (TZVP).[23] Vibrational frequencies were determined by analytical second derivatives of the total electronic energy.[24,25] Thermodynamic properties at 0 and 298 K were computed with the program Viewmol 2.4.[26] Additional coupled-cluster calculations with single, double, and perturbative triple excitations [CCSD(T)] as well as multireference (MR) calculations with the averaged coupled pair functional (ACPF) were performed with MOLPRO 2002.[27] Calculations were performed as single-point energy calculations using the B3LYP/TZVP structures. In these wave-function-based calculations, TZVP basis sets were used first, and then also the TZV basis set as well as Dunning-type basis sets of triple, quadruple, and quintuple quality (cc-pVXZ) were employed. In the case of the MR calculations, the active space comprised seven electrons and seven orbitals.

3. Results

A detailed experimental and theoretical elucidation of the ionization of neutral **1** and the primary fragmentations of the molecular ion $\mathbf{1}^+$ has been reported in a previous paper,[6] and the results are briefly summarized here. Photoionization experiments yield an ionization energy of IE(**1**) = 9.54 ± 0.05 eV and an appearance energy of AE($\mathbf{1}^+ - CH_2O$) = 10.1 ± 0.1 eV for the loss of formaldehyde from the molecular ion ($\mathbf{1}^+ \rightarrow \mathbf{2}^+$; Scheme 1). Some experimental observations already indicated the existence of an alternative route, and theoretical studies revealed that another type of H_2 migration ($\mathbf{1}^+ \rightarrow \mathbf{2a}^+$) can indeed compete efficiently. At elevated energies, also direct V−O bond cleavage takes place to yield a methoxy radical concomitant with the formation of $\mathbf{5}^+$.

Consecutively, the primary dissociation products $\mathbf{2}^+$ and/or $\mathbf{2a}^+$ as well as $\mathbf{5}^+$ first undergo dehydrogenation followed by two sequential losses of neutral formaldehyde or a methoxy radical, respectively, i.e., $\mathbf{2}^+ \rightarrow \mathbf{3}^+ \rightarrow \mathbf{4}^+ \rightarrow VOH^+$, $\mathbf{2a}^+ \rightarrow \mathbf{3a}^+ \rightarrow \mathbf{4a}^+ \rightarrow VO^+$, and $\mathbf{5}^+ \rightarrow \mathbf{6}^+ \rightarrow \mathbf{7}^+ \rightarrow VO^+$ (Scheme 1). Thus, VOH^+ and VO^+ respectively can be considered as the quasi-terminal fragments of the fragmentation sequences; the terminal cationic fragment is atomic V^+.[28] Here, we

(15) Eller, K.; Schwarz, H. *Int. J. Mass Spectrom. Ion Processes* **1989**, *93*, 243.
(16) Engeser, M.; Schröder, D.; Weiske, T.; Schwarz, H. *J. Phys. Chem. A* **2003**, *107*, 2855.
(17) Schröder, D.; Schwarz, H.; Clemmer, D. E.; Chen, Y.-M.; Armentrout, P. B.; Baranov, V. I.; Böhme, D. K. *Int. J. Mass Spectrom. Ion Processes* **1997**, *161*, 175.
(18) Bartmess, J. E.; Georgiadis, R. M. *Vacuum* **1983**, *33*, 149.
(19) Becke, A. D. *J. Chem. Phys.* **1993**, *98*, 5648.
(20) Stephens, P. J.; Derlin, F. J.; Chabalowski, C. F.; Frisch, M. J. *J. Phys. Chem.* **1994**, *98*, 11623.
(21) Ahlrichs, R.; Bär, M.; Häser, M.; Horn, H.; Kölmel, C. *Chem. Phys. Lett.* **1989**, *162*, 165.
(22) Treutler, O.; Ahlrichs, R. *J. Chem. Phys.* **1995**, *102*, 346.
(23) Schäfer, A.; Huber, C.; Ahlrichs, R. *J. Chem. Phys.* **1994**, *100*, 5829.
(24) Deglmann, P.; Furche, F.; Ahlrichs, R. *Chem. Phys. Lett.* **2002**, *362*, 511.
(25) Deglmann, P.; Furche, F. *J. Chem. Phys.* **2002**, *117*, 9535.
(26) http://viewmol.sourceforge.net/.
(27) Amos, R. D.; Bernhardsson, A.; Berning, A.; Celani, P.; Cooper, D. L.; Deegan, M. J. O.; Dobbyn, A. J.; Eckert, F.; Hampel, C.; Hetzer, G.; Knowles, P. J.; Korona, T.; Lindh, R.; Lloyd, A. W.; McNicholas, S. J.; Manby, F. R.; Meyer, W.; Mura, M. E.; Nicklass, A.; Palmieri, P.; Pitzer, R.; Rauhut, G.; Schütz, M.; Schumann, U.; Stoll, H.; Stone, A. J.; Tarroni, R.; Thorsteinsson, T.; Werner, H.-J. MOLPRO, a package of ab initio programs designed by H.-J. Werner and P. J. Knowles, version 2002.1.

attempt to confirm this tentatively assigned dissociation sequence by complementary experimental and theoretical studies. To this end, an understanding of ion fragmentation is approached from the opposite side, that is, an investigation of the formation of larger ions from smaller ones in ion/molecule reactions of mass-selected V-containing cations with appropriate neutral compounds.

3.1. ESI Experiments. In our previous paper,[6] the assignment of the structures of secondary fragment ions remained somewhat ambiguous because, with the lack of data of isomeric ions for comparison, structural assignments based on collision experiments alone are difficult. In the particular case of the vanadium alkoxide ions examined in this study, ESI turns out to offer a useful complementary approach.[29−32]

As proposed in Scheme 1, elimination of formaldehyde from the molecular ion $\mathbf{1}^+$ affords the formal V^{IV} compounds $\mathbf{2}^+$ and/or $\mathbf{2a}^+$, which then eliminate H_2 to afford $\mathbf{3}^+$ and/or $\mathbf{3a}^+$, followed by further losses of formaldehyde. Accordingly, a solution of the bulk V^{IV} compound $OVSO_4$ in water/methanol was subjected to ESI. At soft ionization conditions, characterized by low cone voltages ($U_C = 5-15$ V), monocationic clusters of the formal series $[OV(HSO_4)(CH_3OH)_n]^+$ and $[OV(OCH_3)(CH_3OH)_n]^+$ ($n = 1-3$) are obtained in reasonable abundances; formation of the latter cation can be ascribed to methanolysis of $OVSO_4$. At slightly elevated cone voltages ($U_C = 20-40$ V), these complexes undergo successive fragmentations to yield inter alia ions formally equivalent to some of the fragments emerging from ionized $\mathbf{1}^+$. Upon an increase of U_C to 60−100 V, the cationic species VOH^+ and VO^+ predominate, and finally the atomic V^+ cation is formed ($U_C > 120$ V).

With respect to the consecutive fragmentations of the molecular ion $\mathbf{1}^+$, the CID patterns of the ions derived from the formal $[OV(OCH_3)(CH_3OH)_n]^+$ clusters are of interest. For $n = 3$, loss of methanol is observed exclusively, while competition of water and methanol losses is observed for the cluster with $n = 2$ (not shown). As far as elemental composition is concerned, the species with $n = 1$, $[VC_2H_7O_3]^+$, is identical with structures $\mathbf{2}^+$ and $\mathbf{2a}^+$ proposed to be involved in the fragmentation of $\mathbf{1}^+$. Low-energy CID of the $[VC_2H_7O_3]^+$ ion formed upon ESI gives rise to dehydrogenation followed by elimination of neutral CH_2O at elevated collision energies (Table 1), thus qualitatively matching the fragmentations observed for mass-selected $[VC_2H_7O_3]^+$ generated by dissociative electron ionization of neutral **1** (for details, see ref 6). Note that no more than qualitative agreement can be expected because the CID spectra in the multipole instrument used here apply collision energies of several electronvolts, whereas the previous collision experiments were conducted at kiloelectronvolt energies.[33] Again, and consistent with the results of the previous work, almost exclusive loss of formaldehyde is observed for the $[VC_2H_5O_3]^+$ ion formed upon ESI of $OVSO_4$ in water/methanol under slightly more drastic ionization conditions. Upon a further increase of the cone voltage, also accessible is a $[VCH_3O_2]^+$ cation, which undergoes elimination of formaldehyde at low and additional losses of a methoxy radical at elevated collision energies. Such a behavior points to a structural dichotomy of the $[VCH_3O_2]^+$ species because loss of formaldehyde implies structure $\mathbf{4}^+$, whereas formation of VO^+ is indicative of structure $\mathbf{4a}^+$. The same conclusion was drawn in our previous study of $[VCH_3O_2]^+$ generated by dissociative ionization of **1**. In resuming these results, we conclude that identical ion structures (or at least more or less identical mixtures of isomeric ions) are formed upon dissociative ionization of **1** and ESI of $OVSO_4$ in water/methanol.

Table 1. Product Branching Ratios Listed According to the Mass Differences (Δm)[a] Observed upon CID (Collision Gas: Xe)[b] of Q(1) Mass-Selected Cations Generated by ESI of $OVSO_4$ in Water/Methanol and $OV(OCH_3)_3$ in Pure Methanol, Respectively, and the Characteristic Values $E_{1/2}$ and $b_{1/2}$[c]

			Δm						
	$E_{1/2}$[c]	$b_{1/2}$[c]	−2	−15	−18	−28	−30	−31	−32
$OVSO_4$ in Water/Methanol									
$[VC_2H_7O_3]^+$	1.3	2.5	100	3	2		20		
$[VC_2H_5O_3]^+$	1.5	2.2			5		100		
$[VCH_3O_2]^+$	2.5	1.9					100	2	
	5.0[d]	1.7[d]		1			100	30	
$OV(OCH_3)_3$ in Methanol									
$[VC_2H_6O_3]^+$	1.4	1.8	100				12		3
$[VC_2H_4O_3]^+$	2.0	1.4					100		
$[VCH_2O_2]^+$	5.1	0.6					100		

[a] Given relative to the base peak (100) of the CID products. [b] Data given for $E_{CM} = E_{1/2}$. [c] Unless mentioned otherwise, these parameters ($E_{1/2}$ in eV and $E_{1/2}$ without dimension) refer to the fragmentation, which gives rise to the base peak of the corresponding spectrum. [d] Estimated values for the VO^+ ($\Delta m = -31$) channel.

In addition to the fragmentation patterns, the CID experiments conducted at different collision energies provide semiquantitative information about the ion energetics in terms of $E_{1/2}$ values (see experimental details). Thus, the loss of H_2 from $[VC_2H_7O_3]^+$ is relatively facile ($E_{1/2} = 1.3$ eV), and the elimination of formaldehyde from $[VC_2H_5O_3]^+$ is less energy-demanding ($E_{1/2} = 1.5$ eV) than that from $[VCH_3O_2]^+$ ($E_{1/2} = 2.5$ eV). Again, these findings are consistent with the qualitative conclusions derived from the previous mass spectrometric experiments.

Further insight into ion structures is provided by an investigation of the ion/molecule reactions of the mass-selected species with D_2O and CD_3OD, respectively.[7−9,34] While only the product distributions obtained at a collision energy (E_{lab}) formally set to 0 eV are given in Table 2, it is

(28) Schröder, D.; Engeser, M.; Schwarz, H.; Harvey, J. N. *ChemPhysChem* **2002**, *3*, 584.
(29) Henderson, W.; McIndoe, J. S.; Nicholson, B. K.; Dyson, P. J. *J. Chem. Soc., Chem. Commun.* **1996**, 1183.
(30) Lover, T.; Henderson, W.; Bowmaker, G. A.; Seakins, J. M.; Cooney, R. P. *J. Mater. Chem.* **1997**, *7*, 1553.
(31) Zemski, K. A.; Castleman, A. W., Jr. *J. Phys. Chem. A* **2001**, *105*, 4633.
(32) Waters, T.; O'Hair, R. A. J.; Wedd, A. G. *J. Am. Chem. Soc.* **2003**, *125*, 3384.
(33) Schröder, D. In *Encyclopedia of Mass Spectrometry*; Armentrout, P. B., Ed.; Elsevier: Amsterdam, The Netherlands, 2003; Vol. 1, p 460.
(34) It is to be considered, however, that the ion/molecule reactions used as probes may themselves also induce structural rearrangements. For example, see: (a) Becker, H.; Schröder, D.; Zummack, W.; Schwarz, H. *J. Am. Chem. Soc.* **1994**, *116*, 1096. (b) Beyer, M. K.; Berg, C. B.; Achatz, U.; Joos, S.; Niedner-Schatteburg, G.; Bondybey, V. E. *Mol. Phys.* **2001**, *99*, 699.

Table 2. Product Branching Ratios Listed According to the Mass Differences (Δm)[a] Observed in the Ion/Molecule Reactions[b] of Q(1) Mass-Selected Cations Generated by ESI of $OVSO_4$ in Water/Methanol with D_2O and CD_3OD, Respectively[c]

		Δm														
	reagent	−10	+1	+3	+4	+6	+14	+16	+17[d]	+20	+30	+31	+32	+33	+44	+46
$[VC_2H_7O_3]^+$	D_2O		90							10						
	CD_3OD		5	15	20				60							
	CH_3OCH_3						80									20
$[VC_2H_5O_3]^+$	D_2O	65	5							30						
	CD_3OD					90			10							
	CH_3OCH_3							100								
$[VCH_3O_2]^+$	D_2O		5						80	15						
	CD_3OD			10		2			5				38	45		
	CH_3OCH_3							25				30			15	30
VOH^+	D_2O		30						65	5						
	CD_3OD		5						80[e]					15[f]		
	CH_3OCH_3						10				15	65			10	
VO^+	CD_3OD												100[g]			
	CH_3OCH_3										65	5				30

[a] Given as product branching ratios ($\Sigma = 100$). [b] Data given for $E_{lab} = 0$ eV. [c] While the reagents used had >99.5 atom % D, H/D exchange inside the mass spectrometer lowers the actual degree of deuteration of the hydroxy groups to about 85 atom % D; the CD_3 group of methanol remains unaffected.[d] In all cases, some amount of $\Delta m = +16$ was observed as well but was fully consistent with the H/D exchange of the neutral reagents. [e] Here, use of the labeled reagent is a disadvantage because it cannot be distinguished whether one or both of the isomeric ions $OVOD^+$ and $VOCD_3^+$ (both $m/z = 85$) is formed; see section 3.2. [f] Part if not all of this channel might be ascribed to the secondary reaction of initially formed $VOCD_3^+$ with CD_3OD via O-atom transfer.[8] [g] The primary product $OV(OCD_2)^+$ undergoes rapid ligand exchange with CD_3OD to afford $OV(CD_3OD)^+$.[8]

noted in addition that almost all products rapidly decline at elevated collision energies and all of them disappear above $E_{lab} = 5$ eV. This energy behavior justifies the assignment of the products to those of quasi-thermal ion/molecule reactions.[11,35]

In the reaction of mass-selected $[VC_2H_7O_3]^+$ with D_2O, a single H/D exchange is observed as demonstrated by a mass difference of $\Delta m = +1$. This behavior is consistent with the presence of a hydroxy group in structure $\mathbf{2}^+$ but also is compatible with structure $\mathbf{2a}^+$, in which the methanol ligand could undergo H/D exchange. In addition, some adduct formation with D_2O ($\Delta m = +20$) is observed, a process that is not structurally indicative, however, because both ion structures considered here possess vacant coordination sites. A more complex pattern evolves in the reaction of $[VC_2H_7O_3]^+$ with deuterated methanol. The major pathway corresponds to the addition of CD_3OD concomitant with the loss of HDO ($\Delta m = +36 - 19 = +17$), which is ascribed to methanolysis of the hydroxy group in $\mathbf{2}^+$ to afford the trimethoxyvanadium cation $V(OCH_3)_2(OCD_3)^+$. The structural assignment of the latter is supported by the observation of two consecutive reactions with CD_3OD, which first yield $V(OCH_3)(OCD_3)_2^+$ and then $V(OCD_3)_3^+$ without any hint for the occurrence of partial H/D exchanges (note that only the primary ion/molecule reactions are listed in Table 2). This sequence appears less likely for the isomeric structure $\mathbf{2a}^+$. In addition to methanolysis, also simple H/D exchange ($\Delta m = +1$) as well as degenerate replacement of one methoxy group ($\Delta m = +34 - 31 = +3$) takes place with CD_3OD. The two latter pathways do not help in the structural assignment, however, because their occurrence can be expected for both isomers under debate ($\mathbf{2}^+$ as well as $\mathbf{2a}^+$). Another reaction leads to a formal exchange of an intact methanol molecule ($\Delta m = +36 - 32 = +4$) and might therefore indicate a contribution from the isomeric structure $\mathbf{2a}^+$. However, this mass difference can also be explained by a combination of H/D and CH_3O/CD_3O exchanges of $\mathbf{2}^+$ during the lifetime of the collision complex. We thus conclude that the majority of the $[VC_2H_7O_3]^+$ ions formed upon ESI exhibit structure $\mathbf{2}^+$, with the isomeric ion $\mathbf{2a}^+$ either being present as a minor contribution in the mass-selected ion beam or being accessible via isomerization of the ion/molecule complex formed upon collision with neutral methanol.

The $[VC_2H_5O_3]^+$ cation generated upon ESI readily forms an adduct with D_2O ($\Delta m = +20$) but shows only a little H/D exchange ($\Delta m = +1$), consistent with the assumed presence of a vanadyl unit in structure $\mathbf{3a}^+$. This assignment finds further support by the observed exchange of only one formaldehyde ligand by D_2O ($\Delta m = +20 - 30 = -10$), even at elevated D_2O pressure. In contrast, both H/D scrambling as well as up to two exchanges of formaldehyde and D_2O ligands are expected for the isomeric structure $\mathbf{3}^+$. The presence of a formaldehyde unit in $[VC_2H_5O_3]^+$ is also implied by the reaction with deuterated methanol, in which the major product channel ($\Delta m = +36 - 30 = +6$) can be ascribed to a replacement of CH_2O by CD_3OD. Because structures $\mathbf{3}^+$ and $\mathbf{3a}^+$ both contain a CH_2O ligand, this process is not structurally indicative, however. Only a side reaction (addition of CD_3OD and loss of HDO; $\Delta m = +36 - 19 = +17$) points toward a contribution of the isomeric ion $\mathbf{3}^+$. Accordingly, the majority of the $[VC_2H_5O_3]^+$ ions are attributed to structure $\mathbf{3a}^+$.

As mentioned above, the CID results are inconclusive as far as the structure of $[VCH_3O_2]^+$ ($m/z = 98$) is concerned: the observed loss of formaldehyde implies $HOVOCH_2^+$ ($\mathbf{4}^+$), whereas the formation of VO^+ at high collision energies suggests $OVOCH_3^+$ ($\mathbf{4a}^+$). In this respect, the ion/molecule reactions are quite helpful. With D_2O, only a trace of H/D exchange ($\Delta m = +1$) is observed, whereas the major route involves the addition of D_2O concomitant with loss of HD ($\Delta m = +20 - 3 = +17$). Irrespective of the detailed reaction mechanism, specific loss of HD from the intermediate complex $\mathbf{8}^+$ appears less likely because H/D exchange

(35) Schröder, D.; Schwarz, H.; Schenk, S.; Anders, E. *Angew. Chem.* **2003**, *115*, 5241; *Angew. Chem., Int. Ed.* **2003**, *42*, 5087.

Scheme 2

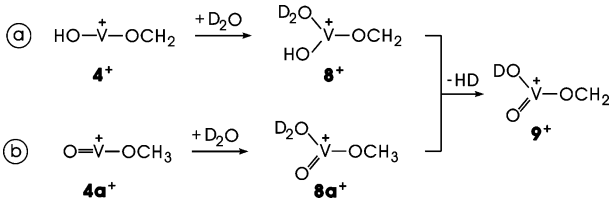

between the hydroxy group and the water ligand is expected to occur as well (Scheme 2a). Instead, a specific expulsion of HD is easily rationalized with structure **8a**$^+$, in which the H atoms of the ionic reactant are in different binding situations than the D atoms of the neutral reactant (i.e., C−H vs O−D bonds; Scheme 2b). Assignment of structure **4a**$^+$ to the $[VCH_3O_2]^+$ ion formed upon ESI also accounts for the inefficient H/D exchange with D_2O, even though the nonnegligible amount of $\Delta m = +1$ observed experimentally may indicate the presence of **4**$^+$ as a minor component or the possibility of a water-induced rearrangement (**4a**$^+ \rightarrow$ **4**$^+$); likewise, the observation of a small percentage of $\Delta m = +6$ in the reaction with CD_3OD may point to traces of structure **4**$^+$, which bears an intact formaldehyde ligand. Further support of structure **4a**$^+$ is lent by the observation of a degenerate exchange of the methoxy unit ($\Delta m = +3$) with CD_3OD. The major channel involves the addition of methanol followed by losses of either D_2 or HD ($\Delta m = +32$ and $+33$). In this case, losses of two isotopologues of H_2 is fully consistent with structure **4a**$^+$ because the putative reaction intermediate corresponds to deuterated **2**$^+$, i.e., $DOV(OCD_3)(OCH_3)^+$, for which competition of HD and D_2 losses is precisely what is expected.

Next, the reactions of VOH^+ formed under harsher ionization conditions are addressed. In addition to the expected H/D exchange occurring with D_2O ($\Delta m = +1$), the addition of D_2O concomitant with loss of HD ($\Delta m = +20 - 3 = +17$) and a trace of adduct formation ($\Delta m = +20$) are observed. Quite interestingly, $\Delta m = +17$ implies the formation of the formal V^{IV} compound $OVOD^+$ at thermal energies, and thus $D(HOV^+-O) \geq 117$ kcal/mol, which corresponds to the dehydrogenation enthalpy of water.[36] The reaction of VOH^+ with CD_3OD inter alia leads to a $[VCD_3O_2]^+$ product ion ($\Delta m = +33$), thereby closing the cycle from VOH^+ to the primary fragments of dissociative ionization of neutral **1**. At elevated cone voltages, ESI of $OVSO_4$ also yields VO^+, which does not show any reaction with D_2O under these conditions,[37] and slowly dehydrogenates CD_3OD to afford $[VCD_2O_2]^+$, thus the deuterated analogue of **7**$^+$ (see below). In a subsequent, rapid reaction, exchange of CD_2O by CD_3OD is observed to yield $[VCD_4O_2]^+$.[7−9]

In addition, some ion/molecule reactions with dimethyl ether, CH_3OCH_3, were examined. For the ions $[VC_2H_5O_3]^+$ and $[VC_2H_7O_3]^+$, formal ligand-exchange reactions lead to the formation of a product ion with $m/z = 144$ in both cases, most probably $OV(OCH_3)(CH_3OCH_3)^+$. Further, variable amounts of association complexes are formed. Most interesting in the present context are the abstractions of a methoxy unit ($\Delta m = +31$) observed for mass-selected $[VCH_3O_2]^+$, VOH^+, and VO^+, implying that the respective $V-OCH_3$ bond strengths are close to or even exceed $D(CH_3O-CH_3) = 84$ kcal/mol. Particularly instructive in this respect is the behavior of VO^+. Figure 1 shows the product yield for the reaction of VO^+ with dimethyl ether as a function of the collision energy. At $E_{CM} = 0$ eV, formal association ($\Delta m = +46$)[38] and loss of methane from the collision complex ($\Delta m = +46 - 16 = +30$) prevail, whereas the fraction of methoxy abstraction ($\Delta m = +31$) is rather low. While the overall product yields rapidly decrease at elevated collision energies, the fraction of $\Delta m = +31$ passes through a maximum. This energy behavior can be regarded as a clear indication that the methoxy abstraction from dimethyl ether by VO^+ is an entropically favorable, but slightly endothermic process.

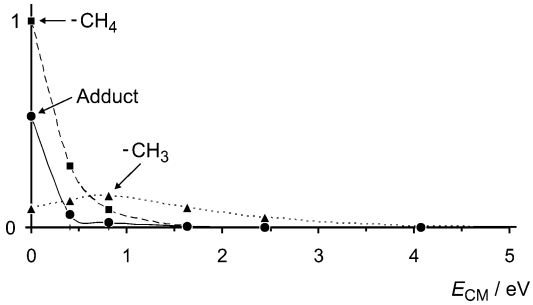

Figure 1. Product-ion branching ratio in the reaction of mass-selected VO^+ with dimethyl ether abundances at different collision energies E_{CM} (in eV). Here three products are observed: the formal adduct a $[VC_2H_6O_2]^+$ (●), the loss of CH_4 leading to $[VCH_2O_2]^+$ (■), and the expulsion of a methyl radical $CH_3^\bullet$ leading to a $[VCH_3O_2]^+$ cation (▲).

Encouraged by the useful information gained from these experiments, the corresponding ions formed upon ESI of **1** dissolved in methanol were investigated briefly. Use of this precursor inter alia provides access to the ions $[VC_2H_6O_3]^+$, $[VC_2H_4O_3]^+$, and $[VCH_2O_2]^+$, corresponding to the elemental compositions of structures **5**$^+$−**7**$^+$ in Scheme 1. Because ion abundances were weaker upon ESI of this neutral precursor, the investigations were limited to CID studies. The dissociation behavior of these ions obtained upon ESI (Table 1) is again in qualitative agreement with the fragmentation patterns observed in the previous sector-field experiments: dehydrogenation prevails for $[VC_2H_6O_3]^+$ and losses of formaldehyde predominate for $[VC_2H_4O_3]^+$ and $[VCH_2O_2]^+$ with VO^+ as the quasi-terminal fragment. The genesis of these ions in ESI can be ascribed to the initial protonation of neutral **1** followed by loss of methanol, i.e., [**1** + H]$^+ \rightarrow$ **5**$^+ \rightarrow$ **6**$^+ \rightarrow$ **7**$^+ \rightarrow VO^+$ (only ionic products are given).

In a more general perspective, it is notable that the types of fragment ions formed upon ESI at elevated cone voltages

(36) Linstrom, P. J., Mallard, W. G., Eds. *NIST Chemistry WebBook*; NIST Standard Reference Database Number 69; National Institute of Standards and Technology: Gaithersburg, MD, July 2001 (http://webbook.nist.gov).

(37) Koyanagi, G. K.; Bohme, D. K.; Kretzschmar, I.; Schröder, D.; Schwarz, H. *J. Phys. Chem. A* **2001**, *105*, 4259.

(38) We note in passing that the rapid exchange of the formaldehyde ligand in $OV(OCH_2)^+$ by CH_3OCH_3 observed in the ICR experiment indicates that part of the signal for $\Delta m = +46$ in Table 2 may be due to consecutive processes.

can be controlled to quite some extent by the valence of the neutral V compound present in solution. Thus, ESI of the V^{IV} compound $OVSO_4$ primarily affords $[VC_mH_nO_o]^+$ cations with an odd number of H atoms *n*, e.g., VOH^+, $[VCH_3O_2]^+$, $[VC_2H_5O_3]^+$, and $[VC_2H_7O_3]^+$, nascent from the V^{II}/V^{IV} redox manifold. In contrast, ESI of the V^V compound $OV(OCH_3)_3$ leads to $[VC_mH_nO_o]^+$ cations with even *n*, thus comprising formal V^{III}/V^V, e.g., VO^+, $[VCH_2O_2]^+$, $[VC_2H_4O_3]^+$, $[VC_2H_6O_3]^+$, and $[VC_3H_{10}O_4]^+$.

3.2. ICR Experiments. Because there is some ambiguity with respect to the integrity of ion structures as well as the precise internal energy content of the ions generated upon ESI at elevated cone voltages,[10,11,39] some complementary experiments using an ICR mass spectrometer are mentioned briefly.[7,8] The particular advantage of the ICR experiments is that ion thermalization can be assumed safely in the present case. Thus, mass-selected VO^+ equilibrated to ambient temperature slowly dehydrogenates methanol to yield $[VCH_2O_2]^+$ (reaction 1) with a reaction efficiency $k_r/k_c = 0.06$,[40] and the consecutive, more rapid reaction 2 then affords $[VCH_4O_2]^+$. Likewise, VOH^+ reacts with methanol to form first $[VCH_3O]^+$ ($k_r/k_c = 0.70$), which then adopts a second O atom in the consecutive reaction with methanol (reactions 3 and 4).

$$VO^+ + CH_3OH \rightarrow [VCH_2O_2]^+ + H_2 \quad (1)$$

$$[VCH_2O_2]^+ + CH_3OH \rightarrow [VCH_4O_2]^+ + CH_2O \quad (2)$$

$$VOH^+ + CH_3OH \rightarrow VOCH_3^+ + H_2O \quad (3)$$

$$VOCH_3^+ + CH_3OH \rightarrow [VCH_3O_2]^+ + CH_4 \quad (4)$$

These results are fully consistent with the ESI measurements described above, and we therefore refrain from any further discussion. The major purpose of the ICR experiments is to confirm that reactions observed in the ESI measurements can be regarded to occur as more or less thermal processes, even though ion generation upon ESI at elevated cone voltages involves multicollisional excitation. We note in passing that the use of unlabeled methanol in the ICR experiments demonstrates that the reaction of VOH^+ with methanol inter alia affords $VOCH_3^+$, while this cannot be concluded safely from the ESI experiments with CD_3OD, where $\Delta m = +17$ could be attributed to loss of either HDO or CHD_3 from the collision complex.

Finally, the reaction of mass-selected VO^+ with dimethyl ether was investigated, which was found to occur with $k_r/k_c = 0.40$. Consistent with the results obtained in the ESI measurement (Table 2), the major route leads to the elimination of methane (reaction 5a) and a minor path is associated with expulsion of a methyl radical (reaction 5b); the branching ratio amounts to 94:6. Investigation of the reaction kinetics under ICR conditions further demonstrates that the formal adduct $[VC_2H_6O_2]^+$ observed in the ESI measurements can at least in part be ascribed to a rapid consecutive reaction of the ionic product $[VCH_2O_2]^+$ of reaction 5a in that a formaldehyde unit is replaced by dimethyl ether (reaction 6).

$$VO^+ + CH_3OCH_3 \rightarrow [VCH_2O_2]^+ + CH_4 \quad (5a)$$

$$\rightarrow [VCH_3O_2]^+ + CH_3^{\bullet} \quad (5b)$$

$$[VCH_2O_2]^+ + CH_3OCH_3 \rightarrow [VC_2H_6O_2]^+ + CH_2O \quad (6)$$

We have not tried to assess whether part of the formal adduct observed in the ESI measurements does indeed correspond to a direct association of VO^+ with dimethyl ether because the pressure in the multipole MS/MS study exceeds that in the ICR experiments by orders of magnitude (10^{-4} vs 10^{-8} mbar). Within the context of the present study, the mere fact that reaction 5b can occur for thermalized VO^+ under ICR conditions is most important because it implies that $D(OV^+-OCH_3)$ is $\geq 84 \pm 3$ kcal/mol, where the latter quantity is the bond energy $D(CH_3O-CH_3)$ in conjunction with the uncertainty associated with a thermal reaction occurring under ICR conditions.[41] Further note that this conclusion is in full agreement with the ESI data described above.

3.3. Theoretical Results on Fragment Ions. The ground states of neutral **1**, the molecular cation $\mathbf{1}^+$, and the primary dissociation products $\mathbf{2}^+-\mathbf{4}^+$ have been described in our previous paper on the ion chemistry of trimethoxyvanadate. Here, we concentrate on the anticipated fragments formed en route to the quasi-terminal fragments VOH^+ and VO^+, thus the minima $\mathbf{1}^+-\mathbf{7}^+$ and, in particular, their energetics as well as spin states.

The structure of the molecular ion $\mathbf{1}^+$ is similar to that of the neutral precursor, except the presence of one elongated V−O bond in the cationic species (Figure 2 and Table 3). H_2 transfer followed by loss of formaldehyde leads to either $\mathbf{2}^+$ or $\mathbf{2a}^+$. The former bears one hydroxy and two methoxy ligands as reflected by the similar V−O bond lengths (r_{VO} = 1.70 and 1.72 Å, respectively), whereas structure $\mathbf{2a}^+$ still bears a vanadyl group and a coordinatively bound methanol molecule, resulting in much more differentiated V−O bond lengths (ranging from 1.57 to 2.01 Å). Both structures can be described as formal V^{IV} compounds and have doublet ground states. The subsequent dehydrogenation leads to structures $\mathbf{3}^+$ and $\mathbf{3a}^+$, respectively. In the transition $\mathbf{2}^+ \rightarrow \mathbf{3}^+ + H_2$, two methoxy groups convert to formaldehyde ligands, which is associated with an elongation of r_{VO} from 1.70 to 1.99 Å and, hence, with a reduction from formal V^{IV} to V^{II}. This change in electron occupation at the metal center also leads to a quartet ground state. In contrast, the dehydrogenation $\mathbf{2a}^+ \rightarrow \mathbf{3a}^+ + H_2$ leaves the formal V^{IV} unchanged, and thus doublet ground states are preserved; here, the oxidation process involves the C atom only, as reflected in the significant shortening of r_{CO} from 1.49 Å in

(39) Schröder, D.; Schwarz, H.; Holthausen, M. C. *J. Phys. Chem. B* **2004**, *108*, 14407.

(40) k_r = experimental rate constant. k_c = gas kinetic collision frequency. Here, k_c is calculated using the capture theory. See: Su, T. *J. Chem. Phys.* **1988**, *89*, 5355 and references cited therein.

(41) Bouchoux, G.; Salpin, J. Y.; Leblanc, D. *Int. J. Mass Spectrom.* **1996**, *153*, 37.

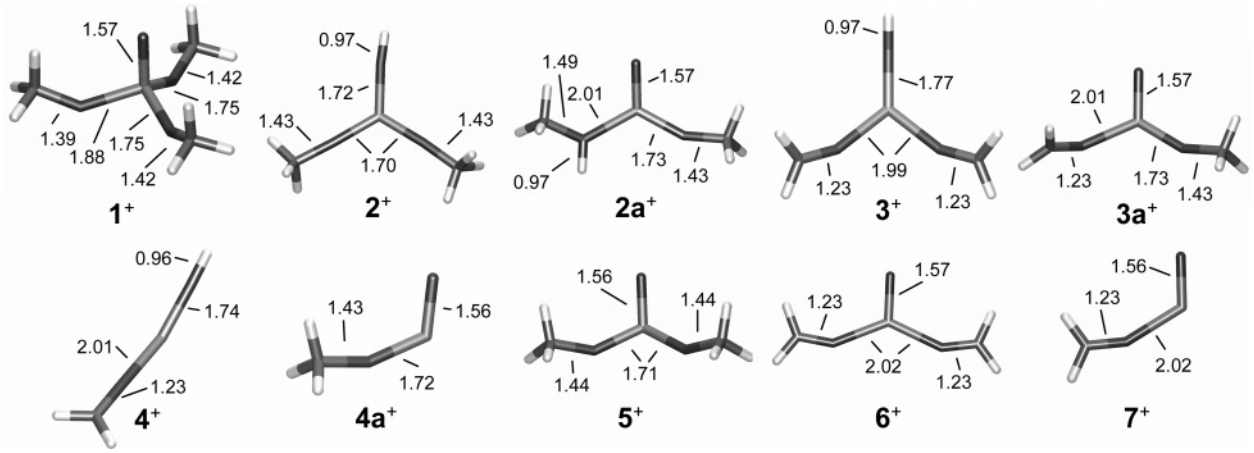

Figure 2. Calculated geometries of structures $\mathbf{1}^+-\mathbf{7}^+$ (bond lengths in Å). Also see Table 3.

Table 3. Selected Structure Parameters of the Ionic Species $\mathbf{1}^+-\mathbf{7}^+$ According to B3LYP Calculations

	$\mathbf{1}^+$	$\mathbf{2}^+$	$\mathbf{2a}^+$	$\mathbf{3}^+$	$\mathbf{3a}^+$	$\mathbf{4}^+$	$\mathbf{4a}^+$	$\mathbf{5}^+$	$\mathbf{6}^+$	$\mathbf{7}^+$
symmetry	C_s	C_1	C_1	C_s	C_1	C_s	C_1	C_s	C_s	C_s
$r(V-{}^1O)$	1.57	1.72	1.57	1.77	1.57	1.74	1.56	1.56	1.57	1.56
$r(V-{}^2O)$	1.88	1.70	2.01	1.99	2.01	2.00	1.72	1.71	2.02	2.02
$r(V-{}^3O)$	1.75	1.70	1.73	1.99	1.73			1.71	2.02	
$r({}^1C-{}^2O)$	1.39	1.43	1.49	1.23	1.23	1.23	1.43	1.44	1.23	1.23
$r({}^2C-{}^3O)$	1.42	1.43	1.43	1.23	1.43			1.44	1.23	
$r({}^1O-H)^a$		0.97	0.97	0.97		0.96				
$\alpha({}^1OV^2O)$	109	121	113	129	112	154	115	111	113	120
$\alpha({}^1OV^3O)$	111	121	118	129	117			111	113	
$\alpha(V^2O^1C)$		177	127	158	149	179	156	145	148	154
$\alpha(V^2O^1C)$		176	154	158	153			145	148	

[a] The various C−H bond lengths differ by less than 0.01 Å and are therefore not listed.

$\mathbf{2a}^+$ to 1.23 Å in $\mathbf{3a}^+$. The losses of formaldehyde ligands from either $\mathbf{3}^+$ or $\mathbf{3a}^+$ are not associated with significant changes of the geometries and spin states in either $\mathbf{4}^+$ or $\mathbf{4a}^+$ or the quasi-terminal VOH^+ fragment in comparison to their precursor ions.

Very similar structural features apply for the fragments resulting from the initial loss of a methoxy radical from $\mathbf{1}^+$. Thus, $\mathbf{5}^+$ bears one short V−O distance associated with the vanadyl moiety and two moderate bond lengths (r_{VO}) of the covalently bound methoxy groups, resulting in a singlet ground state, and hence formal V^V, for $\mathbf{5}^+$. In the subsequent dehydrogenation $\mathbf{5}^+ \rightarrow \mathbf{6}^+ + H_2$, both methoxy groups convert into formaldehyde ligands, which is associated with the expected elongations of r_{VO} as well as a different multiplicity of the ground state, i.e., a triplet, as expected for V^{III}. The further CH_2O losses to afford $\mathbf{7}^+$ and VO^+ are again not associated with significant changes of either the geometries or spin states. One particular issue, to which we return further below, is the possible interconversion of the isomeric species $\mathbf{4}^+$ and $\mathbf{4a}^+$, which differ not only with respect to connectivity but also as far as formal valence is concerned (V^{II} in $\mathbf{4}^+$ vs V^{IV} in $\mathbf{4a}^+$) and hence bear different multiplicities. In addition to a barrier associated with H_2 migration, there might accordingly exist a possible restriction in the interconversion of both isomers due to different spin multiplicities.[42]

To get more detailed insight into this isomerization between structure $\mathbf{4}^+$ and $\mathbf{4a}^+$, the corresponding transition structures (TSs) were also computed in this particular case.

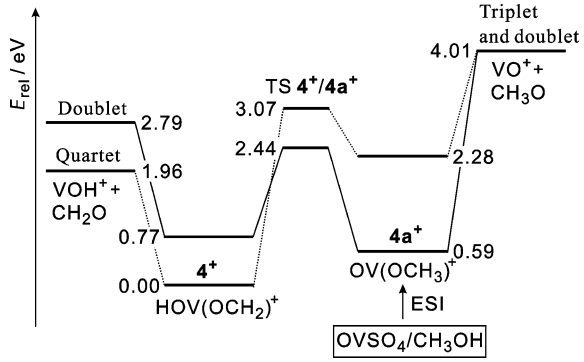

Figure 3. Calculated B3LYP potential-energy surface for the isomerization of the doublet and quartet states of $\mathbf{4}^+$ and $\mathbf{4a}^+$ (energies given at 0 K).

Figure 3 shows a schematic view of the resulting potential-energy surface. Thus, the formaldehyde complex $\mathbf{4}^+$ is predicted as the most stable isomer, having a high-spin (quartet) ground state with the doublet state 0.77 eV higher in energy. For the isomer $\mathbf{4a}^+$, the situation is reversed in that a low-spin (doublet) ground state is preferred, as expected for a V^{IV} compound. Notably, also the low-spin TS is considerably less energy-demanding than the high-spin route.

As far as the energetics of the consecutive fragmentations are concerned, the total energies for all isomers and respective spin states considered are given in Table 4. For a more comprehensive view, however, consideration of the relative energies, E_{rel}, is more suitable (Table 5). Here, the molecular ion $\mathbf{1}^+$ is used as a reference in the E_{rel} columns given for 0 and 298 K. The initial H_2 migration and subsequent loss of formaldehyde is even exothermic for the formation of $\mathbf{2}^+$ and only slightly endothermic for $\mathbf{2a}^+$. As expected for decreasing coordination, the following steps of fragmentation are then more and more energy-demanding. Formation of the quasi-terminal fragments VOH^+ and VO^+ requires 4.55 and 6.60 eV, respectively.

4. Discussion

The different types of mass spectrometric experiments in conjunction with complementary theoretical studies provide valuable insight into the fragmentation behavior of **1** and

(42) For a recent review on the role of spin-forbidden reactions in the gas phase, see: Schwarz, H. *Int. J. Mass Spectrom.* **2004**, *237*, 75.

Table 4. Computed Total Energies (E_{tot} in hartrees),[a] Zero-Point Energies (ZPE in hartrees), and Excitation Energies (T in eV)[b] of Structures $\mathbf{1}^+-\mathbf{7}^+$ and of Some Relevant Fragments[c]

	state	E_{tot}	ZPE	T (eV)[b]
$OV(OCH_3)_3^+$ ($\mathbf{1}^+$)	$^2A''$	−1364.305 39	0.124 51	
$HOV(OCH_3)_2^+$ ($\mathbf{2}^+$)	^2A	−1249.831 57	0.095 77	0.00
	^4A	−1249.757 97	0.092 78	1.92
$OV(OCH_3)(CH_3OH)^+$ ($\mathbf{2a}^+$)	^2A	−1249.809 63	0.098 57	0.00
	^4A	−1249.730 61	0.094 25	2.03
$HOV(OCH_2)_2^+$ ($\mathbf{3}^+$)	^2A	−1248.560 58	0.070 25	0.63
	$^4A''$	−1248.584 29	0.070 95	0.00
	^6A	−1248.453 71	0.066 12	3.42
$OV(OCH_2)(OCH_3)^+$ ($\mathbf{3a}^+$)	^2A	−1248.585 71	0.074 23	0.00
	^4A	−1248.512 35	0.069 87	1.88
$HOV(OCH_2)^+$ ($\mathbf{4}^+$)	^2A	−1134.008 88	0.041 38	0.77
	$^4A''$	−1134.037 23	0.041 40	0.00
	^6A	−1133.908 29	0.036 16	3.37
$OV(OCH_3)^+$ ($\mathbf{4a}^+$)	$^2A'$	−1134.015 51	0.044 37	0.00
	^4A	−1133.953 62	0.039 63	1.56
$OV(OCH_3)_2^+$ ($\mathbf{5}^+$)	^1A	−1249.187 68	0.087 02	0.00
	^3A	−1249.132 01	0.082 44	1.39
$OV(OCH_2)_2^+$ ($\mathbf{6}^+$)	$^1A'$	−1247.948 97	0.062 06	0.65
	$^3A''$	−1247.972 13	0.061 25	0.00
	$^5A'$	−1247.869 92	0.059 97	2.48
$OV(OCH_2)^+$ ($\mathbf{7}^+$)	$^1A'$	−1133.385 17	0.032 00	0.79
	$^3A''$	−1133.413 83	0.031 78	0.00
	^5A	−1133.320 25	0.030 68	2.52
VOH^+	$^2A''$	−1019.441 54	0.011 16	0.83
	$^4A''$	−1019.471 79	0.011 07	0.00
	$^6A'$	−1019.353 68	0.009 84	3.18
VO^+	$^3\Sigma^-$	−1018.850 40	0.002 56	
CH_2O	$^1A_1$	−114.490 02	0.026 59	
CH_3O	$^2A'$	−115.036 87	0.036 10	
H_2	$^1\Sigma_g^+$	−1.172 89	0.010 06	

[a] B3LYP/TZVP. [b] Given relative to the respective electronic ground state. [c] For the selected geometric data of the different isomers, see Table 3.

the associated energetics. In fact, the experimental and theoretical results merge with each other within reasonable error margins all the way from neutral **1** to the quasi-terminal fragments VOH^+ and VO^+. The consistency thus achieved about the ion energetics allows us to address the remaining problems in more detail.

4.1. Thermochemistry. For neutral **1**, Adler et al. indirectly determined the values $\Delta_fH_{298}(\mathbf{1})_g = -222$ and -228 kcal/mol, respectively,[43] of which we take the average $\Delta_fH_{298}(\mathbf{1}) = -225 \pm 3$ kcal/mol as well as the experimental $IE(\mathbf{1})_g = 9.54 \pm 0.05$ eV as anchoring values.[41] Two other anchors from the end of the fragmentation sequence are provided by the cations VO^+ and VOH^+, for which accurate thermochemical data are available (Table 6).[44] These extremes can now be used to link the computed thermochemistry from the neutral molecule **1** to the quasi-terminal ionic fragments VO^+ and VOH^+, respectively. This comparison thereby allows us to probe the performance of the computational method employed for the description of redox processes and rearrangements occurring in mononuclear, gaseous V compounds.

To this end, consider the Δ_fH_{298} column in Table 5. In the evaluation of the values given, $\Delta_fH_{298}(\mathbf{1}^+)$ is treated as a floating parameter in conjunction with the computed relative energies (at 298 K) using neutral **1** as well as the quasi-terminal dissociation asymptotes $VOH^+ + H_2 + 3CH_2O$ and $VO^+ + CH_3O^\bullet + H_2 + 2CH_2O$ as anchors for a least-squares fit (Table 6). Comparison with the reference data (Δ_fH_{ref}) shows pleasing agreement between experiment and theory within less than ±2 kcal/mol, and in combination with the uncertainty of the anchors, we arrive at an error of ±4 kcal/mol.

The computed energetics can further be cross-checked by the thermochemical implications of the ion/molecule reactions described above; in this respect, an error of ±3 kcal/mol is assigned to the thermal processes observed under ESI and ICR conditions,[6] unless mentioned otherwise. Most insightful in this respect are the dehydrogenation of methanol and O_2 transfer, respectively, as well as the methoxy abstraction from dimethyl ether (eqs 1, 4, 5b, and 7−9).

$$VO^+ + CH_3OH \rightarrow [VCH_2O_2]^+ + H_2 \quad (1)$$

$$VOCH_3^+ + CH_3OH \rightarrow [VCH_3O_2]^+ + CH_4 \quad (4)$$

$$VO^+ + CH_3OCH_3 \rightarrow [VCH_3O_2]^+ + CH_3^\bullet \quad (5b)$$

$$[VCH_3O_2]^+ + CH_3OCH_3 \rightarrow [VC_2H_6O_3]^+ + CH_3^\bullet \quad (7)$$

$$[VCH_3O_2]^+ + CH_3OH \rightarrow [VC_2H_5O_2]^+ + CH_2O \quad (8)$$

$$[VC_2H_5O_3]^+ + CH_3OH \rightarrow [VC_2H_7O_3]^+ + CH_2O \quad (9)$$

The occurrence of reaction 1 at thermal energies implies $D(OV^+-OCH_2) \geq 22$ kcal/mol, which is the dehydrogenation enthalpy of methanol, thus leading to an upper limit of $\sum\Delta_fH_{298} \leq 129 \pm 4$ kcal/mol for $[VCH_2O_2]^+ + CH_3O^\bullet + H_2 + CH_2O$. The corresponding entry in Table 5 ($\sum\Delta_fH_{298} = 106.5$ kcal/mol) indicates that $D(V^+-OCH_2)$ is much larger (44.7 kcal/mol) than the lower limit of ≥22 kcal/mol derived from the ion/molecule reaction. Likewise, observation of reaction 4 in combination with $D(V^+-OCH_3) = 98 \pm 10$ kcal/mol and the thermochemical data given in Table 6 implies $\sum\Delta_fH_{298} \leq 102 \pm 11$ kcal/mol for $[VCH_3O_2]^+ + 2CH_2O + H_2$, which clearly allows the formation of both isomers $\mathbf{4}^+$ and $\mathbf{4a}^+$ in Table 5 (58.3 and 74.6 kcal/mol, respectively). The experimental results further suggest that methoxy abstraction in reaction 5b is a slightly endothermic process (see above), suggesting $\sum\Delta_fH_{298} \geq 68 \pm 4$ kcal/mol for $[VCH_3O_2]^+ + 2CH_2O + H_2$. Accordingly, lower and upper limits are derived: $68 \pm 4 \leq \sum\Delta_fH_{298}([VCH_3O_2]^+ + 2CH_2O + H_2) \leq 102 \pm 11$ kcal/mol. The combination of these brackets with reaction 7 further suggests an upper limit $\sum\Delta_fH_{298} \leq 58 \pm 11$ kcal/mol for $[VC_2H_6O_3]^+ + CH_3O^\bullet$. Finally, the occurrence of reaction 8 implies $\sum\Delta_fH_{298} \leq 80 \pm 4$ kcal/mol for $[VC_2H_5O_3]^+ + CH_2O + H_2$, and formal exchange of formaldehyde by methanol in reaction 9 implies $\sum\Delta_fH_{298} \leq 40 \pm 6$ kcal/mol for $[VC_2H_7O_3]^+ + CH_2O$. In summary, the occurrence of all of these ion/molecule reactions at thermal energies is fully consistent with the thermochemical data predicted in Table 5, and the results are also represented in Figure 4. In addition, also the trends of the $E_{1/2}$ values given in Table 1 fully agree with the theoretical predictions. Hence, we conclude that the DFT

(43) Adler, B.; Bieräugel, I.; Lachowicz, A.; Thiele, K.-H. *Z. Anorg. Allg. Chem.* **1977**, *431*, 227.
(44) Armentrout, P. B.; Kickel, B. L. In *Organometallic Ion Chemistry*; Freiser, B. S., ed.; Kluwer: Dordrecht, The Netherlands, 1995; p 1.

Table 5. Relative Energies (E_{rel} in eV)[a] and Sums of the Heats of Formation ($\sum\Delta_f H_{298}$ in kcal/mol) of Several Consecutive Fragmentation Processes of $\mathbf{1}^+$

	state[b]	$E_{rel,0}$ [eV]	$E_{rel,298}$ [eV]	$\sum\Delta_f H_{298}$[c] [kcal/mol]	$\sum\Delta_f H_{ref}$ [kcal/mol]
$OV(OCH_3)_3^+$ ($\mathbf{1}^+$)	^2A	0.00	0.00[d]	−3.8	−5.0[e]
$HOV(OCH_3)_2^+$ ($\mathbf{2}^+$) + CH_2O	$^2A/^1A_1$	−0.50	−0.46	−14.4	
$OV(OCH_3)(CH_3OH)^+$ ($\mathbf{2a}^+$) + CH_2O	$^2A/^1A_1$	0.17	0.19	1.2	
$HOV(OCH_2)_2^+$ ($\mathbf{3}^+$) + CH_2O + H_2	$^4A''/^1A_1/^1\Sigma_g^+$	1.12	1.24	24.3	
$OV(OCH_2)(OCH_3)^+$ ($\mathbf{3a}^+$) + CH_2O + H_2	$^2A/^1A_1/^1\Sigma_g^+$	1.17	1.27	26.0	
$HOV(OCH_2)^+$ ($\mathbf{4}^+$) + $2CH_2O$ + H_2	$^4A''/^2{}^1A_1/^1\Sigma_g^+$	2.59	2.72	58.3	
$OV(OCH_3)^+$ ($\mathbf{4a}^+$) + $2CH_2O$ + H_2	$^2A/^2{}^1A_1/^1\Sigma_g^+$	3.27	3.36	74.6	
VOH^+ + $3CH_2O$ + H_2	$^4A''/^3{}^1A_1/^1\Sigma_g^+$	4.55	4.69[f]	104.3	105.8[f]
$OV(OCH_3)_2^+$ ($\mathbf{5}^+$) + $CH_3O^\bullet$	$^1A'/^2A'$	2.16	2.16	46.0	
$OV(OCH_2)_2^+$ ($\mathbf{6}^+$) + $CH_3O^\bullet$ + H_2	$^3A''/^2A'/^1\Sigma_g^+$	2.90	3.00	65.4	
$OV(OCH_2)^+$ ($\mathbf{7}^+$) + $CH_3O^\bullet$ + H_2 + CH_2O	$^3A''/^2A'/^1\Sigma_g^+/^1A_1$	4.68	4.78	106.5	
VO^+ + $CH_3O^\bullet$ + H_2 + $2CH_2O$	$^3\Sigma\angle/^2A'/^1\Sigma_g^+/^2{}^1A_1$	6.60	6.72[e]	151.2	151.0[f]

[a] B3LYP/TZVP data at 0 K relative to $\mathbf{1}^+$; values at 298 K include enthalpic corrections. [b] Only electronic ground states are included. [c] Fitted values derived from the sums of the heats of formation at 298 K with an error of ±4 kcal/mol; see the text. [d] The absolute difference between 0 and 298 K amounts to 0.38 eV. [e] Derived from $\Delta_f H(\mathbf{1}) = -225$ kcal/mol (Table 6) and IE(**1**) = 9.54 eV taken from ref 6. [f] According to the literature thermochemistry (Table 6), the difference between VOH^+ + CH_2O and VO^+ + $CH_3O^\bullet$ amounts to 1.96 ± 0.17 eV, which compares nicely with the computed difference of 2.03 eV.

Table 6. Heats of Formation (in kcal/mol)[a] of Species Used in the Data Analysis

	$\Delta_f H_{298}$		$\Delta_f H_{298}$
V^+	277.8 ± 1.8[b]	O	59.56 ± 0.02[b]
VO^+	198.8 ± 3[c]	OH	9.40 ± 0.05[b]
VOH^+	183.6 ± 4[d]	H_2O	−57.80 ± 0.01[b]
$OV(OCH_3)_3$	−225 ± 3[e]	CH_2O	−25.95 ± 0.11[b]
H_2	0[b]	$CH_3O^\bullet$	4.1 ± 0.9[b]
$CH_3^\bullet$	35.0 ± 0.1[b]	CH_3OH	−48.07 ± 0.05[b]
CH_4	−17.89 ± 0.01[b]	CH_3OCH_3	−43.99 ± 0.12[b]

[a] Values given for gaseous species at 298 K. [b] Taken from the NIST database (ref 36) or derived from values given therein. [c] Derived using $D_0(V^+-O) = 5.99 \pm 0.10$ eV (Clemmer, D. E.; Elkind, J. L.; Aristov, N.; Armentrout, P. B. *J. Chem. Phys.* **1991**, *95*, 3387). [d] Derived using $D_0(V^+-OH) = 4.50 \pm 0.15$ eV (ref 44). [e] Average of the data given in ref 43.

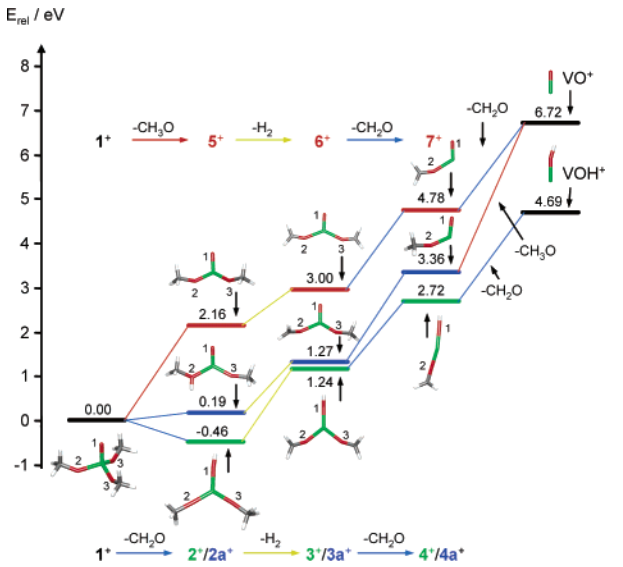

Figure 4. Calculated energetics (in eV) from the cation $\mathbf{1}^+$ to the quasi-terminal fragments VO^+ and VOH^+. Also see Table 5.

applied is able to describe the thermochemistry of the V−O species discussed here from the neutral precursor **1** all the way to the quasi-terminal fragments VO^+ and VOH^+.

4.2. Structures of $[VCH_3O_2]^+$ Cations. Reviewing the experimental and theoretical findings, the structure of the $[VCH_3O_2]^+$ species remains somewhat ambiguous. Thus, most experiments described above point toward structure $\mathbf{4a}^+$: preferred loss of $CH_3O^\bullet$ at higher collision energies, almost negligible H/D exchange in the reaction with D_2O, and degenerate CH_3O/CD_3O exchange with CD_3OD. The prevalence of CH_2O loss in low-energy CID can simply be ascribed to the thermochemical preference of this channel (Table 5) and therefore cannot be considered as structurally indicative. The same conclusion evolves from a comparison of the metastable ion and collisional activation spectra of $[VCH_3O_2]^+$ generated by dissociative electron ionization of **1**. Further, the fact that VOH^+ is able to dehydrogenate water to yield $OVOH^+$ (see above), for which no low-valent isomer is possible, implies that the V^{IV} oxidation state required in $\mathbf{4a}^+$ is accessible at thermal energies. In contrast, theory predicts $\mathbf{4}^+$ to be considerably more stable than $\mathbf{4a}^+$. Nevertheless, the bracketed energetics would fit with both isomers (see above).

There exist two alternative explanations for this discrepancy between experiment and theory. On the one hand, the mass spectrometric measurements might accidentally lead to a preferential formation of the less stable isomer $\mathbf{4a}^+$ under the experimental conditions chosen, as was already indicated in Figure 3. This scenario is, in fact, not too unlikely given the finding that theory predicts dehydrogenation of the primary fragments (i.e., $\mathbf{2}^+ \rightarrow \mathbf{3a}^+$ or $\mathbf{2a}^+ \rightarrow \mathbf{3a}^+$) and subsequent loss of a formaldehyde ligand ($\mathbf{3a}^+ \rightarrow \mathbf{4a}^+$) to proceed on the doublet surface, whereas the sequence involving the isomers $\mathbf{2}^+-\mathbf{4}^+$ requires a change in multiplicity to a quartet spin. As previous evidence indicates that spin inversion is ineffective in the case of some V-containing ions,[45−48] the consecutive fragmentation might therefore indeed lead to $\mathbf{4a}^+$ rather than the more stable isomer $\mathbf{4}^+$. Likewise, methanolysis of the V^{IV} compound $OVSO_4$ in the ESI experiments may preferentially lead to species having a $OVOCH_3^+$ core. In fact, we may indeed encounter the rare situation that two different mass spectrometric approaches both lead to the preferential formation of a less stable isomer

(45) Kretzschmar, I.; Schröder, D.; Schwarz, H.; Rue, C.; Armentrout, P. B. *J. Phys. Chem. A* **1998**, *102*, 10060.
(46) Harvey, J. N.; Diefenbach, M.; Schröder, D.; Schwarz, H. *Int. J. Mass Spectrom.* **1999**, *182/183*, 85.
(47) Rue, C.; Armentrout, P. B.; Kretzschmar, I.; Schröder, D.; Harvey, J. N.; Schwarz, H. *J. Chem. Phys.* **1999**, *110*, 7858.

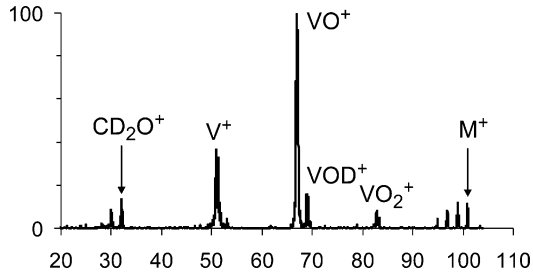

Figure 5. NR mass spectrum of mass-selected $[VCD_3O_2]^+$ generated by EI of $(CD_3O)_3VO$. We note in passing that the assigned formulas are fully supported by analogous experiments conducted with mass-selected $[VCH_3O_2]^+$.

because of kinetic control, most probably as a result of a spin restriction operative in the present case. On the other hand, the theoretical description of the isomers **4**$^+$ and **4a**$^+$ may be somewhat unbalanced. Specifically, **4**$^+$ can be considered as an ion/dipole complex, which can be assumed to be reasonably described with DFT, whereas the formally high-valent vanadium(IV) oxide **4a**$^+$ may exhibit pronounced electron-correlation effects as well as multi-reference character, which may not be treated adequately with B3LYP.[28,49] For this reasoning, some extraploratory studies of **4**$^+$ and **4a**$^+$ were performed using high-level wave-function-based methods. In the corresponding CCSD(T) as well as ACPF calculations, the energy difference between isomers **4**$^+$ and **4a**$^+$ somewhat decreases in favor of an enhanced stabilization of the formally high-valent species **4a**$^+$, yet the stability order of both isomers does not change in comparison with the prediction of B3LYP (Table S1 in the Supporting Information). Hence, it is concluded that the formal V^{II} compound $HOV(OCH_2)^+$, **4**$^+$, is the most stable $[VCH_3O_2]^+$ isomer. Moreover, the comparable results obtained with these different computational approaches imply that the theoretical description of the $[VCH_3O_2]^+$ surface is reasonable and that accordingly the less stable isomer **4a**$^+$ is indeed sampled in the experiments.

Complementary information about structures **4**$^+$ and **4a**$^+$ can further be provided by an additional experimental approach. Specifically, mass-selected $[VCD_3O_2]^+$ generated by EI of $(CD_3O)_3VO$ was subjected to an NR experiment.[12,13] In such an experiment, the cation is first neutralized in a high-energy collision and after a time delay on the order of microseconds reionized again. The mere observation of a recovery ion due to intact $[VCD_3O_2]^+$ in the corresponding NR spectrum (Figure 5) confirms that the corresponding neutral counterpart $[VCD_3O_2]$ has a minimal lifetime in the microsecond regime. Moreover, it is of quite some importance that electron transfer in NR experiments can be considered to occur as a vertical process, in which the corresponding Franck−Condon factors play an important role.[12,13] With regard to previous NR studies of transition-metal complexes,[50−52] several conclusions about the ion structure can further be extracted from the NR spectrum. At first, the intense VO^+ signal suggests the presence of a preformed vanadyl unit in the cation and hence structure **4a**$^+$ rather than **4**$^+$. This proposal is fully consistent with the VO_2^+ fragment additionally observed in the NR spectrum because it can evolve from **4a**$^+$ via loss of a methyl radical, whereas formation of VO_2^+ from **4**$^+$ would require multiple bond cleavages. In contrast, VOD^+ is formed with much weaker abundance, even though this fragment is expected to be formed efficiently from the neutral species **4**. The pattern of CD_nO^+ cations ($n = 0-3$) is also consistent with the presence of a methoxy group in the precursor cation, hence structure **4a**$^+$, because dissociative reionization of neutral $CD_3O^•$ formed upon dissociation of **4a** is likely to occur, whereas the signal for CD_3O^+ is expected to be rather weak.[53] In conclusion, the NR experiment further supports the conjecture that dissociative electron ionization of neutral **1** predominantly leads to structure **4a**$^+$ rather than the more stable isomer **4**$^+$.

5. Conclusions

A combination of various experimental and theoretical approaches allows a rather comprehensive description of the thermodynamics involved in the ionization and successive fragmentation of trimethoxyvanadate(V), **1**, from the neutral compound to the quasi-terminal fragment ions VOH^+ and VO^+. According to the analysis pursued here, the accuracy of the computational predictions is on the order of ±4 kcal/mol, which is sufficient for the description of chemical processes with these species. This finding is of particular importance because it confirms that the DFT method used here can adequately describe redox reactions of gaseous V compounds.

Furthermore, the experimental and theoretical findings suggest a high preference of V/O systems to maintain a high oxidation state of V, either V^{IV} or V^V, and indicate that spin interconversion is less probable for V-containing ions compared to the gas-phase reactions of the late 3d transition metals.[39,45−48] At least in the gas phase, spin restrictions may therefore crucially influence the chemistry of V compounds and therefore affect product branching ratios to a larger extent than was expected on the basis of thermochemical considerations alone.

Acknowledgment. Continuous financial support by the Sonderforschungsbereich 546, the Deutsche Forschungsgemeinschaft, the Fonds der Chemischen Industrie, and the Gesellschaft von Freunden der Technischen Universität Berlin is gratefully acknowledged.

Supporting Information Available: Table S1 containing computed total energies of isomers **4** and **4′** and their energy differences at several theoretical levels. This material is available free of charge via the Internet at http://pubs.acs.org.

IC060150W

(48) Engeser, M.; Schlangen, M.; Schröder, D.; Schwarz, H.; Yumura, T.; Yoshizawa, K. *Organometallics* **2003**, *22*, 3933.
(49) For a related example, see: Brönstrup, M.; Schröder, D.; Kretzschmar, I.; Schwarz, H.; Harvey, J. N. *J. Am. Chem. Soc.* **2001**, *123*, 142.
(50) Schröder, D.; Sülzle, D.; Hrusák, J.; Böhme, D. K.; Schwarz, H. *Int. J. Mass Spectrom. Ion Processes* **1991**, *110*, 145.
(51) Schröder, D.; Bärsch, S.; Schwarz, H. *Chem. Phys. Lett.* **1999**, *309*, 407.
(52) For a recent review, see: Zagorevskii, D. V. *Coord. Chem. Rev.* **2002**, *225*, 5.
(53) Aschi, M.; Harvey, J. N.; Schalley, C. A.; Schröder, D.; Schwarz, H. *J. Chem. Soc., Chem. Commun.* **1998**, 531.